PAMC: POSTURE ALIGNMENT METHOD BASED ON CRBM FOR CAMERA ROBOT SYSTEM

Jingjie HE[1], Wenjing ZHANG[2], Feng XU[3,*]

By acquiring the posture information of the rigid body with markers on the gripper frame, the camera motion on the robot flange can be controlled remotely. The essential step of posture alignment in teleoperation is to calibrate the transformation matrix of the robot base coordinate system and the world coordinate system of the optical tracking system. In this paper, a novel Posture Alignment Method Based on the Customized Rigid Body with Markers (PAMC) was proposed, which was an automatic, accurate and quick method to complete the posture alignment for related coordinate systems without non-systematic errors. PAMC was applied to teleoperation for the camera robot based on the customized rigid body with markers and optical tracking system. The comparative experiments prove that PAMC is better than manual method, with more stable, more flexible physical setting for reference coordinate system, and shorter operation time-consuming. Meanwhile, PAMC is more suitable for camera robot teleoperation than the existed automatic method due to arbitrary calibration posture and collision avoidance.

Keywords: Camera Robot; Teleoperation; Posture Alignment; Eye-Hand Calibration

1. Introduction

The optical tracking system (OTS) captures the marker position with an optical camera. A General Rigid Body with Markers (GRBM) consists of three or four markers. One GRBM represents a Coordinate System (CS) in OTS [1]. Robot teleoperation is an important enhancement of human operability [2-4]. It has many applications in the fields such as the medical treatment and working in dangerous environments [5-8].

1.1 The Camera Robot Teleoperation System

For the camera robot application, a camera is treated as the end-effector. The attitude of the camera is aligned with the gripper frame. A GRBM is mounted on the gripper frame. When moving the gripper frame, the camera at the end of the

[1] Artificial Intelligence Research Institute, Beijing Institute of Petrochemical Technology, 102600, China.
[2] Artificial Intelligence Research Institute, Beijing Institute of Petrochemical Technology, 102600, China.
[3] School of Information and Communication Engineering, University of Electronic Science and Technology of China, Chengdu 611731, China, e-mail: 0020200021@bipt.edu.cn

manipulator is driven to reproduce the trajectory of the gripper frame in real-time [9,10], as shown in Fig. 1. The GRBM is shown in a green box; the gripper frame is shown in a yellow box; the mobile manipulator is shown in a red box; and the camera is shown in a blue box.

The posture of GRBM captured by the OTS is described relative to either the CS defined in the optical hardware or another GRBM. The method of another GRBM as reference CS is more accurate than optical hardware as reference CS [11]. So, in the camera robot system, the world CS is represented by a GRBM. The world CS or the reference CS is named as WoR CS.

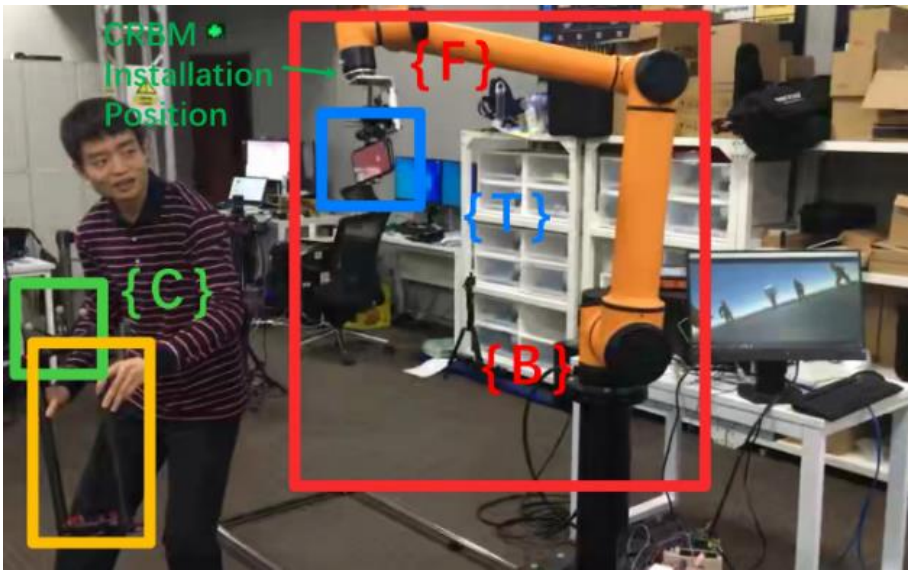

Fig. 1. The camera robot teleoperation system.

1.2 Current Alignment Method

The essential step of posture alignment between the CS of the robot end-effector and the CS of GRBM in OTS, was to find the transformation relationship between the robot base CS and the WoR CS of OTS. A calibration method was proposed in [12]. The GRBM representing the WoR CS was placed on the corner of table, and the manipulator was placed on the table. By these actions, the attitude of WoR CS was set to align with the robot base CS manually. Then by general measurement tools, the posture from the robot base CS to WoR CS was achieved.

The disadvantages of this manual method were as follows. First, the transformation matrix between WoR CS and robot base CS included non-systematic error, and there were not appropriate physical measuring feature points, which was hard to measure by general measurement tools. Second, when transformation matrix was determined, the OTS devices could not be moved. If the robot or optical tracking camera was moved accidentally, it was required to be

measured again. Otherwise, an accident might occur. In studio environment, it was a common occurrence that the camera robot moved to another place for shooting requirements. So, the calibration method should be easy to implement.

The current automatic eye-hand calibration methods included Tsai-Lenz [13], NAVY [14], INRIA [15] and Dual Quaternion [16]. Tsai-Lenz was a standard method. It worked on most calibration attitudes. But in some special calibration attitudes it lost efficacy. Wang Y. [17] and Wang L. [18] proposed the optimization algorithms on the calculation part of the calibration method. The shortage of calibration methods was not solved yet, so the calibration attitudes was constraint in some situations.

In this paper, an automatic, quick and accurate calibration method for teleoperation systems was proposed, named as Posture Alignment Method Based on the Customized Rigid Body with Markers (PAMC). The PAMC was achieved by the Customized Rigid Body with Markers (CRBM) without non-systematic error. The manual method and Tsai-Lenz method were selected to compare with PAMC.

In the first part, the structure of the Camera Robot Teleoperation System (CRTS) was introduced. In the second part, the mathematical derivation of PAMC was discussed. In the third part, the manual method, PAMC and Tsai-Lenz were used to achieve calibration task. By comparing the coefficient of variation, posture deviation and operation time, the performance in terms of stability and time-consuming was analyzed.

2. Posture Alignment Method Based on the CRBM

2.1 The CSs in CRTS

The CSs of the CRTS were shown in Fig. 1. {W} was the WoR CS of OTS, which could be placed in any position where the GRBM of WoR could be captured by optical tracking cameras. {C} was the CS of GRBM. {B} was the CS of robot base. {F} was the CS of the flange at the end of robot. {T} was the CS of camera. The origin of {T} was on the center point of the lens.

2.2 Mathematical Derivation of PAMC

The transformation chain in CRTS was shown in Fig. 2.

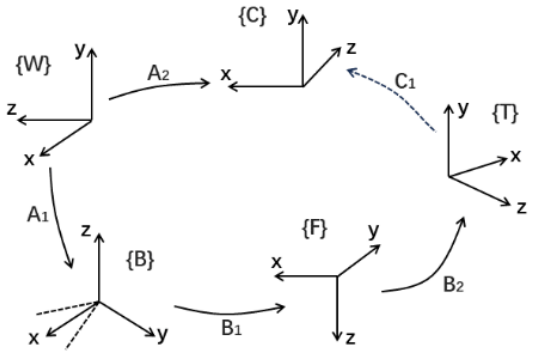

Fig. 2. Transformations of CRTS.

$\boldsymbol{A}_x$, $\boldsymbol{B}_x$, and $\boldsymbol{C}_x$ were 4×4 homogeneous transformation matrices, in which a 3×3 $\boldsymbol{R}$ submatrix representing rotation, and a 3×1 $\boldsymbol{P}$ submatrix representing position.

During the teleoperation of the camera robot, the movement of {C} was reproducing to {T} in real-time. The photographer was only focus on controlling the gripper frame, that was, the posture of GRBM. From a mathematical model perspective, the attitude of {T} and {C} should be aligned at any time, and a fixed position deviation existed for the origin of two CSs.

1) $\boldsymbol{A_1}$ was Known: Assumed $\boldsymbol{A}_1$ had been determined, we had,

$$\boldsymbol{A}_2 = \boldsymbol{A}_1 \cdot \boldsymbol{B}_1 \cdot \boldsymbol{B}_2 \cdot \boldsymbol{C}_1 \tag{1}$$

There was a certain posture deviation between {T} and {C}, denoted as $\boldsymbol{C}_1$. During teleoperation procedure, it was expected that the attitude of {T} and {C} kept aligned, as shown in Fig. 2. The essential step was to determine $\boldsymbol{B}_1$, which represented joint state of robot. Taking $\boldsymbol{B}_1$ as the target, by the inverse kinematic solution, the command values of each joint were calculated.

When {T} and {C} were aligned, $\boldsymbol{B}_1$ was calculated as follows,

$$\boldsymbol{B}_1 = {\boldsymbol{A}_1}^{-1} \cdot \boldsymbol{A}_2 \cdot (\boldsymbol{B}_2 \cdot \boldsymbol{C}_1)^{-1} \tag{2}$$

According to the laws of Lie groups and Lie algebras, the inverse of the transformation matrix was obtained by matrix transpose and multiply operation. Therefore, the calculation of Formula (2) could be finished in real-time.

2) Calibration for $\boldsymbol{A_1}$: The difficulty to calibrate $\boldsymbol{A}_1$ was as follow. First. It was hard to find a physical feature representing {B} posture on robot. There was not any physical marking point for {B}. It was worse that the origin of {B} was inside the robot hardware structure, or in the hollow of the robot base. With this condition, the origin and the orthogonal axis direction of {B} could not be measured by common tools. Second, there was not a physical feature representing {C} posture

on GRBM. Even with physical feature, the pose deviation from the flange to the feature point was difficult to measure with ordinary length measurement tools.

The solution was based on CRBM. CRBM consisted of not only the optical markers and rigid body, but also the mechanical structure that was assembled to robot end flange. Specifically, the posture of CRBM captured by OTS software was consistent with its hardware feature by registering the positions of markers on CRBM to OTS software appropriately. To distinguish from GRBM, CRBM was recorded as {Tc} instead of {C}. As a result, the transformation $\boldsymbol{B}_3$ from {Tc} to {F} was determined by precise mechanical structure size, as shown in Fig. 3.

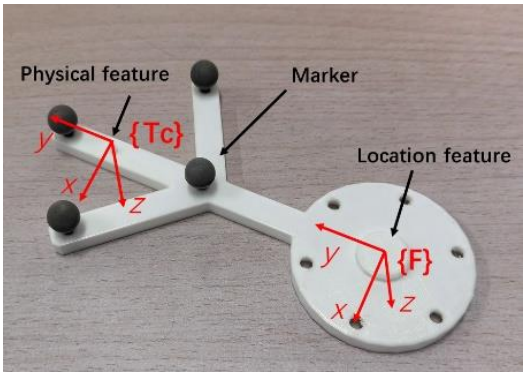

Fig. 3. The CS of CRBM.

The transformation of $\boldsymbol{A}_3$ relative to {W} was read from OTS software. Then the transformation chain of CRTS was shown in Fig. 4.

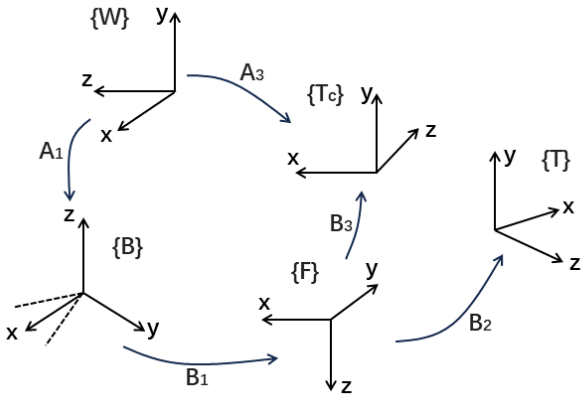

Fig. 4. The transformation chain includes CRBM.

From Fig. 4, we had,

$$\boldsymbol{A}_3 = \boldsymbol{A}_1 \cdot \boldsymbol{B}_1 \cdot \boldsymbol{B}_3 \tag{3}$$

Thus,

$$\boldsymbol{A}_1 = \boldsymbol{A}_3 \cdot (\boldsymbol{B}_1 \cdot \boldsymbol{B}_3)^{-1} \tag{4}$$

In PAMC, CRBM needed to be manufactured precisely. The mechanical positioning of the flange and CS posture of the CRBM in OTS software should be considered during the design procedure. The advantage of this method was that the posture parameters in $\boldsymbol{A}_1$ was calibrated without any actions. In studio scenario, once the transformation of {W} to {B} was determined, camera teleoperation could be implemented.

3. Comparative Experiment

Realman manipulator and FusionTrack500 OTS were used. For automation of the calibration process, a dynamic link library worked on Ubuntu system was developed for FusionTrack500 OTS. The CRBM position and attitude could be read directly by code.

3.1 Manual VS PAMC

The target of the experiment was to calibrate the transformation between the robot base CS, {B}, and world reference GRBM, {W}. Two methods were used for calibration. The first was the manual calibration method. The second was PAMC.

1) **Manual Calibration Method:** The robot was fixed. The exact position of origin of {B} could not be obtained. The attitudes of two CSs were aligned manually. Specifically, the attitude of alignment accuracy was based on human vision. The position deviation was measured by a general measurement tool without physical features, as shown in Fig. 5.

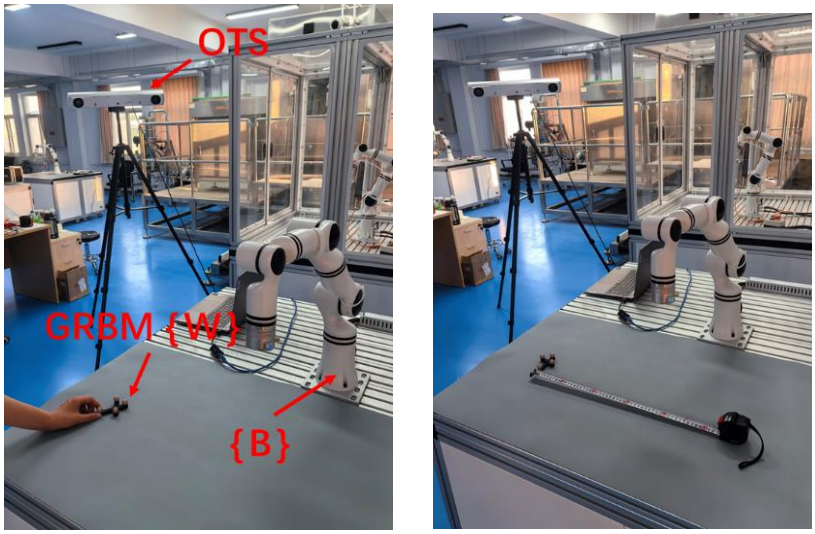

(a) Attitude alignment. (b) General measurement tool.

Fig. 5. Manual calibration method.

There was not ground truth for the manual calibration results. The coefficient of variation of data statistics could be obtained. According to PAMC mathematical analysis, the calibration results of PAMC were better treated as calibration ground truth.

Fifteen people were selected for an independent calibration procedure. The major non-systematic error in the calibration process was the parallelism judgement visually and general measurement.

2) PAMC Method: The CRBM was made as shown in Fig. 3. The transformation was,

$$B_3 = \begin{bmatrix} 1 & 0 & 0 & 0 \\ 0 & 1 & 0 & 100 \\ 0 & 0 & 1 & -3.5 \\ 0 & 0 & 0 & 1 \end{bmatrix} \tag{5}$$

CRBM was installed on the end flange of the robot with the threaded connection, as shown in Fig. 6. The cylindrical protrusion with rounded corner on the CRBM was mainly used for positioning. The rounded corner was used to install easily. This positioning structure ensured that the installation part of the CRBM was concentric with the end flange of the robot. After this, the threaded was used to fix the CRBM and the robot flange. An ini type file which described the geometry relationship between markers and {Tc} was registered in OTS. Then the CRBM could be captured as a rigid body with one attitude and one position in OTS.

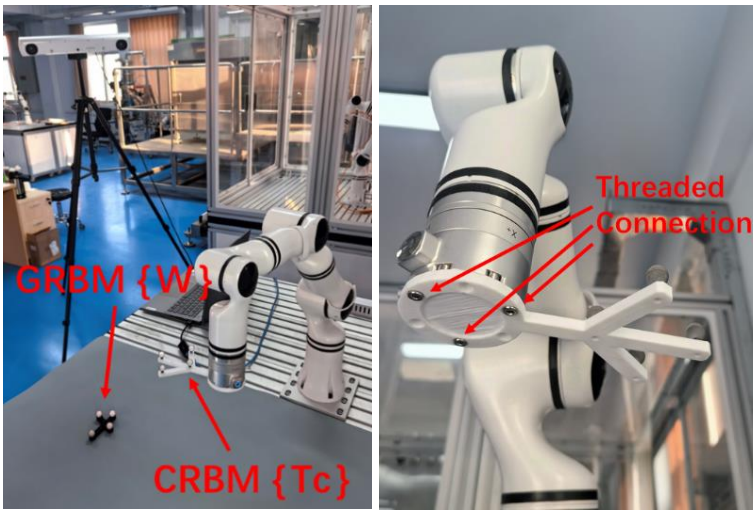

Fig. 6. PAMC calibration method.

The transformation matrix, $\boldsymbol{B}_1$, of {F} relative to {B} could be read directly from robot system. The transformation matrix, $\boldsymbol{A}_3$, of {Tc} relative to {W} could be read directly from OTS. Then $\boldsymbol{A}_1$ could be calculated by Formula (4).

When the marker was passive for infrared, the measurement accuracy of FusionTrack500 optical track system was ±0.3mm. The localization accuracy of the robot was ± 0.05 mm. Therefore, the mean value of each measured data by PAMC could be taken as the ground truth value in this comparison experiment.

$$\Delta p = \| P_{b1PAMC} - P_{b1MANUAL} \| \tag{6}$$

$$\Delta \theta = 2 \cdot arccos(q_{b1PAMC} \cdot q_{b1MANUAL}) \tag{7}$$

By Formula (6), the position deviation of each measurement was calculated. The rotation matrix was expressed in quaternions and the attitude deviation between two poses was calculated by Formula (7). Then the mean and coefficient of variation (CV) were calculated for multiple sets of data.

In multiple PAMC tests, the robot was moved by software of robot firmware as shown in Fig. 7.

Fig. 7. Robot movement control panel.

By data analysis, the results were shown in Fig. 8. The area of triangle of PAMC smaller, the performance of PAMC better. The following conclusions can be reached.

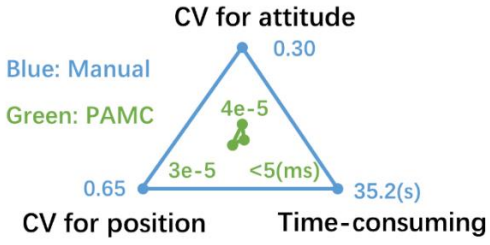

Fig. 8. Performance comparison.

- The data measurement stability (CV) of PAMC is significantly higher than that

of the manual calibration method, whose magnitude order is 3-4 for attitude and position. The high stability of data measurement indicates the high reliability of PAMC.

- The time-consuming fluctuation (standard deviation) of manual calibration method is large, which is 6.4. There was a significant difference of operation time for some people. The average time is 35.2s. The time consuming of PAMC is almost not fluctuated. The average time is less than 5ms.

On the other hand, the {W} in PAMC could be place in any posture. In the Manual method, it was necessary to measure angle for each principal axis if {W} was place in any posture. This would lead to more time-consuming and fluctuation of measurement data.

To sum up, PAMC was faster and more efficient.

3.2 Tsai-Lenz VS PAMC

Tsai-Lenz and PAMC were both automatic. In processing of two methods, the posture of {W} was fixed. For eye-to-hand system, the essential solution was the equation $\boldsymbol{AX} = \boldsymbol{XB}$ by Tsai-Lenz method.

1) Calibration Process: PAMC calibration was executed 20 times with different posture of camera robot configurations. Tsai-Lenz calibration was executed 20 times in which one calibration included 2 target postures. Since Tsai-Lenz was working without information of $\boldsymbol{B}_2$, any GRBM could be installed in any pose on the end of flange.
2) Performance Comparison: The CVs for attitude and position in $\boldsymbol{A}_1$ for two methods were compared.

- Both methods are stable. The CSs of two methods are very small. There is a difference of absolute value for two calibration results, as shown in Fig. 9. The mean of position and attitude angle of Tsai-Lenz was treated as the ground truth for position and attitude angle. There were many factors that lead to differences of absolute value. But the main factor was the low manufacturing accuracy of CRBM which was made by cheap rapid prototyping material. It was possible to compensate for current defects through high-precision machining technology.
- For time-consuming, two target postures are required by Tsai-Lenz at least. One target posture is required by PAMC. PAMC cost less than 5ms. Tai-Lenz costs about 9.6s for one calibration. Based on CRBM, PAMC took almost no time.

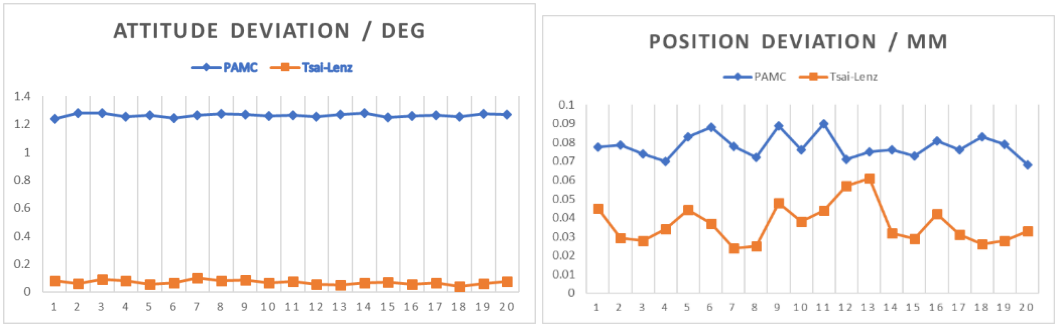

(a) Attitude deviation. (b) Position deviation.

Fig. 9. PAMC VS Tsai-Lenz.

3) The usage condition comparison:

- Since PAMC is not based on $\boldsymbol{AX} = \boldsymbol{XB}$, the error of PAMC is independent of the calibration attitude. When the axes of {C} and {B} are parallel, even as the X axis of {C} and Z axis of {B}, the significant error of Tsai-Lenz cannot be ignored, which lead to failure.
- Both methods can calibrate the posture information. The time-consuming of CRBM is much shorter than Tsai-Lenz. More importantly, PAMC work with no movement for calibration in most situation.

4. Conclusions

In this paper, we proposed PAMC to calibration in teleoperation of camera robot based on OTS.

In PAMC, the accuracy of manufacturing and installation for CRBM used for calibration is quite high. The advantage is that PAMC does not require paying attention to the calibration postures. Meanwhile, the camera robot can get the posture alignment without any action, which lead to avoid collisions between the camera and the studio environments.

The calibration procedure of PAMC is automatic, accurate and fast, which does not contain non-systematic error. PAMC can be used in other applications based on the OTS.

At last, the comparative experiments show that PAMC is better than manual method in many fields, including stability and time-consuming. Even the high-precise mechanism is expensive, it is more suitable for camera robot teleoperation application scenario than the existed automatic calibration methods.

Acknowledgements

This work was supported by the Climbing Program Foundation from Beijing Institute of Petrochemical Technology (Project No. BIPTAAI-008), and

Beijing Municipal Education Commission Science and Technology General Project (Project No. KM202310017001).

REFERENCES

[1]. Optitrack. “Quick start guide: Getting started,” 2021, https://v30.wiki.optitrack.com/index.php-?title=Quick Start Guide: Getting Started.

[2]. M. Rauscher, M. Kimmel, and S. Hirche, “Constrained robot control using control barrier functions,” In IEEE/RS International Conference on Intelligent Robots & Systems, 2016.

[3]. J. Rebelo and A. Schiele, “Master-slave mapping and slave base placement optimization for intuitive and kinematically robust direct teleoperation,” In International Conference on Control, 2012.

[4]. D. Cruzortiz, I. Chairez, and A. Poznyak, “Robust control for master - slave manipulator system avoiding obstacle collision under restricted working space,” IET Control Theory & Applications, 2019.

[5]. B. Hannaford, J. Rosen, D. W. Friedman et al., “Raven-ii: An open platform for surgical robotics research,” IEEE Transactions on Biomedical Engineering, vol. 60, no. 4, pp. 954–959, 2013.

[6]. O. Mohareri, C. Schneider, and S. Salcudean, “Bimanual telerobotic surgery with asymmetric force feedback: A davinci surgical system implementation,” In IEEE/RS International Conference on Intelligent Robots & Systems, pp. 4272–4277, 2014.

[7]. Z. Chen, F. Huang, W. Chen et al., “Rbfnn-based adaptive sliding mode control design for delayed nonlinear multilateral telerobotic system with cooperative manipulation,” IEEE Transactions on Industrial Informatics, vol. 16, no. 2, pp. 1236–1247, 2020.

[8]. Z. Chen, F. Huang, C. Yang, and B. Yao, “Adaptive fuzzy backstepping control for stable nonlinear bilateral teleoperation manipulators with enhanced transparency performance,” IEEE Transactions on Industrial Electronics, vol. 67, no. 1, pp. 746–756, 2020.

[9]. J. He, C. Wang, and S. Wang, “Research into a control schema for camera robot capable of artistic creation,” In 2020 International Conference on Cultureoriented Science & Technology (ICCST), 2020.

[10]. J. He, “A position-level global optimization inverse kinematic solution algorithm for dual redundant robots based on motion characteristics,” Mathematical Problems in Engineering, 2018, https://doi.org/10.1155/2018/9167837.

[11]. Atracsys. “Fusiontrack 500 user manual,” 2020, https: //www.sunya.biz/downloads.html.

[12]. X. Yu, T. Xu, J. Bai, L. Ou, and W. Lu, “Data acquisition system of teaching robot based on optical motion capture,” CN109848964A, 2019.

[13]. R. Y. Tsai and R. K. Lenz, “A new technique for fully autonomous and efficent 3d robotics hand/eye calibration,” IEEE Transactions on Robotics & Automation, vol. 5, no. 3, pp. 345–358, 1989.

[14]. F. C. Park and B. J. Martin, “Robot sensor calibration: solving ax = xb on the euclidean group,” IEEE Transactions on Robotics & Automation, vol. 10, no. 5, pp. 717–721, 2002.

[15]. Horaud, Radu, Dornaika and Fadi, “Hand-eye calibration,” International Journal of Robotics Research, 1995.

[16]. A. Dekel, L. Hrenstam-Nielsen, and S. Caccamo, “Optimal least-squares solution to the hand-eye calibration problem,” 2020.

[17]. Wang Ying et al, "A New Method for Robot Hand Eye Calibration Based on Linear Models," Pattern Recognition and Artificial Intelligence, 18.4 (2005): 5.

[18]. Wang Long, Min Huasong, "Dual Quaternion Hand Eye Calibration Algorithm Based on LMI Optimization," Machine Tool and Hydraulic, 49.21 (2021): 7.